Acta orthop. scand. *52*, 481–490, 1981

FATIGUE BEHAVIOR OF ADULT CORTICAL BONE: THE INFLUENCE OF MEAN STRAIN AND STRAIN RANGE*

DENNIS R. CARTER, WILLIAM E. CALER, DAN M. SPENGLER & VICTOR H. FRANKEL

Orthopaedic Research Laboratories, Department of Orthopaedic Surgery, Massachusetts General Hospital and Harvard Medical School, Boston and Department of Orthopaedics, University of Washington School of Medicine, Seattle, USA

Uniaxial fatigue tests were conducted of devitalized cortical bone specimens machined from human femora. Specimens were tested at strain ranges from 0.005 to 0.010 under physiologic loading rates. The influence of compressive, zero, and tensile mean strains on fatigue life and on the stress/strain histories during fatigue were examined. Results showed that bone fatigue is a gradual damage process accompanied by a progressive increase in hysteresis and a loss of bone stiffness. The total number of cycles to fatigue failure was influenced only by the total strain range and was not affected by mean strain. Bone was shown to have extremely poor fatigue resistance. Fully reversed cyclic loading to one half of the yield strain caused fatigue fracture in 1000 cycles.

Biological implications. The bone regions which experience the highest strain ranges *in vivo* generally have a compressive mean strain. The results of this study indicate that mechanical fatigue damage accumulates more rapidly in these "compressive" areas than in "tensile" areas of bone.

Key words: bone microdamage; bone remodeling; fatigue fracture; strain; stress

Accepted 18.i.81

Previous fatigue studies of devitalized cortical bone specimens have been conducted with bending loads and/or high loading frequencies (Carter & Hayes 1976, Carter et al. 1976, Evans & Lebow 1957, Evans & Riolo 1970, Gray & Korbacher 1974, King & Evans 1967, Lafferty 1978, Lease & Evans 1959, Swanson et al. 1971). The data derived from these studies result in optimistic estimates of bone material fatigue resistance since 1) in most materials, fatigue resistance is greater in bending than in uniaxial loading, and 2) viscoelastic materials (such as bone) are more fatigue resistant at high loading rates than at lower, more physiologic loading rates. Carter et al. (1977) and Carter & Spengler (1978) showed that uniaxial fatigue tests of bone conducted at physiologic loading rates result in much lower fatigue lives than tests conducted in a bending mode at high loading rates. Lafferty (1978) showed that loading frequency has a significant influence on the fatigue lives of rotating bending bone specimens.

Bone fatigue fracture *in vivo* is a complex phenomenon in which mechanical damage and biological repair processes play an important role (Carter & Hayes 1977a, Carter & Hayes 1977b, Chamay & Tschantz 1972, Freeman et al. 1974, Nash 1966, Prather et al. 1977, Radin 1972). If bone fatigue microdamage accumulates at a slow rate, biological remodeling may act to repair the damage and maintain the structural integrity of the bone. On the other hand, the creation of fatigue microcracks may initiate an osteoclastic

* Supported by NIH Grant AM 27117

0001-6470/81/050481-10 $02.50/0

response in a manner analogous to that observed in the first stage of fracture healing. The subsequent removal of bone tissue by osteoclasts in a region of bone which continues to be loaded with high cyclic stresses may accelerate the accumulation of fatigue damage.

The biological response of bone to fatigue microdamage may be influenced by the type of damage which is introduced. Carter & Hayes (1977b) demonstrated that fatigue microdamage is markedly different for bone subjected to repeated tensile stresses than repeated compressive stresses. Tensile fatigue tends to cause failure at osteon cement lines and results in debonding of osteons from the surrounding interstitial bone. Compressive fatigue, however, causes the formation of diffuse shear microcracks throughout the bone which are oblique to the loading direction. The findings of Carter & Hayes are consistent with *in vivo* compressive damage observed by Chamay & Tschantz (1972).

A clear understanding of the material response of devitalized bone tissue to fatigue loading can provide insights into the *in vivo* bone fatigue process. In this study we examined the uniaxial fatigue characteristics of human femoral cortical bone under strain control at physiologic loading rates. The influence of strain range and mean strain on the total number of cycles to fatigue failure were investigated. The mechanical events associated with fatigue damage accumulation were observed. The fatigue data of this study are related to strain histories which may be expected *in vivo*.

MECHANICAL TESTING

The femoral mid-diaphyses of two male (age 82 and 84 years) and two female (age 51 and 53 years) subjects were obtained from autopsy. A band saw was used to cut the bones into slabs of bone approximately 6 × 6 × 37 millimeters which were oriented with the long axis of the femur. These bone pieces were turned on a lathe using a standard specimen template to produce the bone specimens to be fatigue tested (Figure 1). The central sections of the specimens had a diameter of 3 millimeters and a gauge length of 10 millimeters. All machining was conducted while the specimens were sprayed with an oil-water suspension. The bone tissue was not allowed to dry at any time during specimen preparation. Specimens were stored in air-tight containers at –20°C prior to mechanical testing.

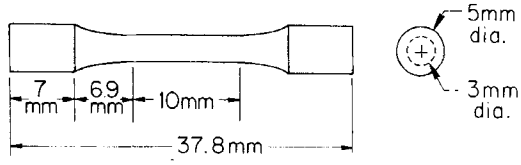

Figure 1. Geometry of bone specimens.

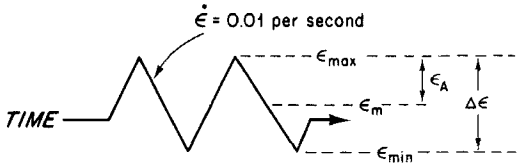

Figure 2. Strain loading history and parameter definitions.

During mechanical testing, the specimens were enclosed in a high humidity environmental chamber with an ambient temperature of 37°C. The tests were conducted with a closed-loop MTS electrohydraulic test system with a built-in digital function generator. The specimens were wrapped with water-soaked tissue paper with a 10 millimeter gauge length extensometer attached to the central test section. Specially designed grips with a Wood's metal reservoir provided excellent grip alignment so that reversed loading (tension to compression) could be performed.

Previous fatigue tests of bone have shown that greater data scatter results with testing under stress control than under strain control (Carter & Spengler 1978). Fatigue testing in this study was therefore conducted with constant strain ranges from 0.005 to 0.010 and mean strains of 0.002, 0.0, and –0.002 (Table 1). Consistent with usual conventions, strain range ($\Delta\varepsilon$) is defined as twice the strain amplitude (ε_A), and mean strain (ε_m) is one half of the sum of the maximum strain (ε max) and minimum strain (ε min). A triangular strain program with a constant strain rate ($\dot{\varepsilon}$) of 0.01 per second was used (Figure 2). This strain rate is consistent with those expected *in vivo* during severe exercise conditions. Since the loading frequency (ν) equals $\dot{\varepsilon}/2\Delta\varepsilon$,

Table 1. Fatigue test groups

		Strain Range $\Delta\varepsilon$					
		0.005	0.006	0.007	0.008	0.009	0.010
Mean Strain ε_m	–0.002	0	5	5	4	6	5
	0.0	0	6	4	4	5	6
	+0.002	5	5	5	4	5	0

the loading frequency was between 0.5 and 1.0 Hertz. The strain vs. time and stress vs. time histories were monitored on a two-channel strip chart recorder. In addition, stress vs. strain curves at selected fatigue cycles were recorded on an oscilloscope.

In applying the strain histories to the specimens, the appropriate mean strain was introduced and maintained on the specimens for 10 to 20 seconds. Very minimal (if any) stress relaxation occurred during the initial 2 seconds of this period, and therefore, a steady state condition was reached prior to the initiation of fatigue cycling. The cyclic loading was superimposed on the specimens and was controlled by a digital function generator.

Since bone fatigue is a gradual, progressive process, there is some arbitrariness in defining fatigue failure (Carter & Hayes 1977a, Carter & Spengler 1978). In this paper we have used a stiffness criterion to define the number of cycles to failure. Total failure was said to have occurred when the total stress range ($\Delta\sigma$) was diminished to 70 percent of the range recorded on the first loading cycle ($\Delta\sigma_0$) (Salkind 1972). The value of 70 percent was chosen since, for specimens tested at all three mean strains, this stiffness value correlated well with the appearance of a distinct bend in the stress vs. strain curve. Other researchers have used the appearance of such a bend as an indication of major crack formation in polymeric materials (Johnson 1973).

Ten additional specimens were subjected to monotonic tensile tests to failure and the stress vs. strain curves were recorded. Testing was conducted at a strain rate of 0.01 per second to allow a direct comparison with the fatigue data.

Bone porosity

After mechanical testing, two small cylinders from each specimen were cut off using a diamond saw and placed in acetone. One was later used in density and ash fraction measurements and the other was embedded in a plastic resin and polished for examination of the cross section in a reflected light microscope. The porosity of the embedded specimens was determined using a point counting technique (Underwood 1970). The point counting mesh used provided 6358 points per square centimeter of bone. Since lacunae were not included in the point counting precedure, a correction factor was used to estimate the true porosity (P) (including lacunae) from the measured porosity (Pm). This adjustment was based on our measured estimates of 300 lacunae per square millimeter of bone tissue. We also estimated that the sectioned lacunae had an average area of 50 square micrometers. These estimates were consistent with the histomorphometric results of other researchers (Baud 1976).

$$Pm = \frac{\text{area of pores (excluding lacunae and canaliculi)}}{\text{Total Area}}$$

$$P = \frac{\text{area of pores (excluding canaliculi)}}{\text{Total Area}}$$

$$P = Pm + (300)\ (0.00005)\ (1-Pm)$$
$$P = Pm + 0.015\ (1-Pm)$$

Wet density

The bone wet density (ϱ) was defined as

$$\varrho = \frac{\text{mass of wet sample}}{\text{bulk volume of wet sample}}$$

The bulk volume of the wet sample was determined by the water displacement technique. The sample was degassed with a vacuum pump while submerged in water and the submerged mass determined with an analytical balance. The sample was then removed from the water and the surface was blotted with a laboratory tissue. The mass of the wet sample was then measured. The bulk volume of the wet sample (in cubic centimeters) was taken as the difference between the submerged mass and the wet mass (expressed in grams) (Mueller et al. 1966).

Ash fraction

After density measurements had been made, the bone samples were dried in acetone for 3 days, in air for 1 day, and then placed in a 60°C oven for 6 hours. The samples were weighed dry, then ashed in a muffle furnace at 600°C for 12 hours and weighed again. The ash fraction (α) was calculated as:

$$\alpha = \frac{\text{weight of ash}}{\text{weight of dry bone}}$$

RESULTS

Bone physical properties

The means and standard deviations for porosity, ash fraction and wet density of the bone specimens are presented in Table 2. Histological examination confirmed that all specimens were comprised of bone with a secondary Haversian

Table 2. Bone physical properties

	n	Porosity (%)	Ash Fraction %	Wet Density (g/cm^3)
Tensile Specimens	10	14.5	66.4	1.77
(S.D.)		(5.6)	(0.5)	(0.09)
Fatigue Specimens	68	13.7	64.9	1.86
(S.D.)		(5.1)	(1.4)	(0.07)

Table 3. Tensile specimen mechanical properties

Mechanical Property		Mean	(S.D.)
Elastic Modulus E (GPa)		17.5	(1.9)
Yield, Strain* (mm/mm)	ε_y	0.0068	(0.0004)
	ε_y'	0.0084	(0.0005)
Ultimate Strain	ε_u	0.0157	(0.0038)
Yield Stress* (MPa)	σ_y	129	(11)
	σ_y'	121	(11)
Ultimate Stress (MPa)	σ_u	140	(12)

* ε_y and σ_y determined by method of Reilly & Burstein (1975)
ε_y' and σ_y' determined by 0.2 percent offset method

microstructure. The ash measurements ranged from 61 to 68 percent.

Tensile testing

The monotonic tensile tests to failure resulted in stress/strain curves similar to those of Reilly & Burstein (1975). In tabulating the results of these data, we considered two definitions of yielding. Reilly & Burstein chose to define yield stress and strain by the point of intersection of the tangents to the curve in the elastic and inelastic regions. In many engineering materials, the yield point is determined by the 0.2 percent offset method (Timoshenko & Young 1968). Yield properties were measured using both of these techniques. The means and standard deviations for elastic modulus, yield stress and strain, and ultimate strength are tabulated in Table 3.

Fatigue testing

The influence of mean strain, maximum strain, and strain range on the total number of cycles to failure is shown in Figures 3 and 4. Both figures incorporate log-log scales to be consistent with standard practices for analyzing fatigue data. The data of Figure 3 suggest that the maximum cyclic strain experienced by bone tissue is not a good predictor of fatigue life for specimens tested with different mean strains. In general, for two specimens tested to the same maximum strain, the

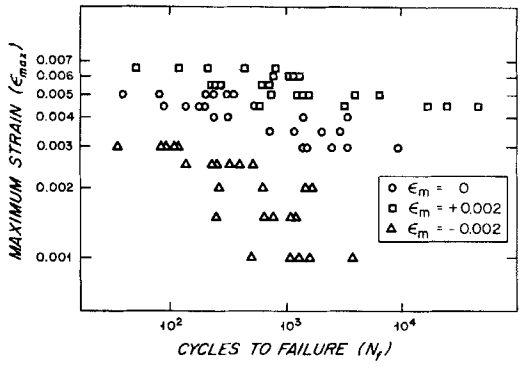

Figure 3. Influence of maximum strain on fatigue cycles to failure for specimens tested at different mean strains.

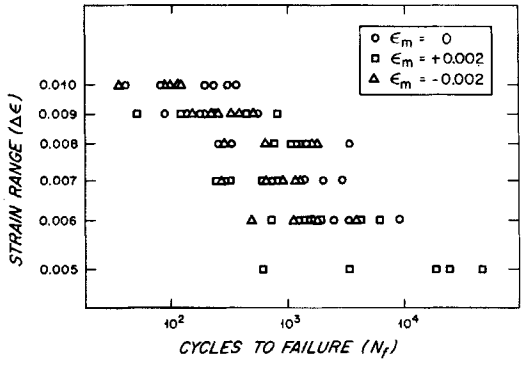

Figure 4. Influence of strain range of fatigue cycles to failure for specimens tested at different mean strains.

specimens tested with smaller strain range will have the longer fatigue life.

Figure 4 demonstrates the relationship between total strain range ($\Delta\varepsilon$) and the total number of cycles to failure (N_f). Regression analysis of these data revealed no statistically significant influence of mean strain on the log ($\Delta\varepsilon$) vs. log (N_f) curves. The data for all the fatigue specimens were therefore grouped together and a least squares regression curve was calculated.

$$\log N_f = A \log\Delta\varepsilon + B. \quad (1)$$

The calculated value of A was –5.342 (S.E. = 0.594) and the value of B was –8.532. Using these values with equation (1) to estimate log N_f for any of the tested specimens, the standard error of the estimate is 0.4085. These data indicate that the relationship between N_f and $\Delta\varepsilon$ can be expressed as:

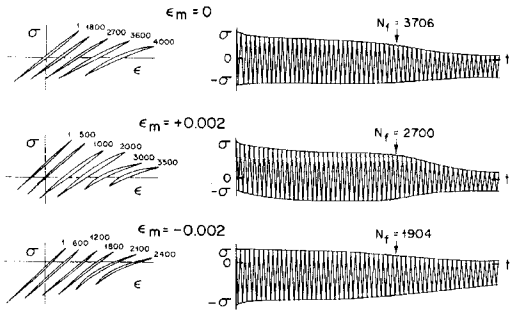

Figure 5. Stress/strain curves and stress histories for specimens tested at different mean strains with a strain range of 0.006.

$$N_f = 2.94\Delta\varepsilon^{-5.342} \times 10^{-9} \quad (2)$$

or

$$\Delta\varepsilon = 0.025\ N_f^{-0.187}. \quad (3)$$

Although the specimens tested at the three different mean strains failed in approximately the same number of cycles, the stress/strain behavior during fatigue loading was distinctly different in the three test groups. Figure 5 illustrates stress/strain curves recorded at selected loading cycles during fatigue loading for typical specimens tested with a strain range of 0.006 and mean strains of 0.0, +0.002, and −0.002. Also shown are curves showing the stress vs. time histories. The mean number of cycles to failure for these specimens (based on Equation 1) was 2147 with a total time to failure of 2587 seconds.

Specimens tested with a zero mean strain exhibited a gradual, progressive decrease in the tensile stress amplitude during fatigue loading. A similar though distinctively less severe decrease in compressive stress amplitude was observed. Hysteresis in the stress/strain curve also increased progressively. Greater hysteresis was observed on the tensile side of the curve than on the compressive side. Late in the fatigue life, the decrease in stress amplitude with each loading cycle became more pronounced, suggesting a rapid accumulation of fatigue damage. This phenomenon coincided with the appearance of a bend in the recorded stress/strain curves and marked hysteresis. At failure the tensile stress amplitude for the specimens in this test group was decreased to 61 per cent (S.D. 10) of the tensile stress amplitude recorded on the first loading cycle. The compressive stress amplitude was decreased to 87 per cent (S. D. 6) of the initial compressive amplitude (Figure 5).

Specimens tested with a tensile mean strain of +0.002 exhibited a sharp decrease in tensile stress amplitude during the first 5–15 loading cycles. This was followed by a more gradual decrease in tensile stress amplitude throughout most of the fatigue life. The compressive stress amplitude increased progressively during fatigue loading reaching a maximum of approximately 154 percent of the initial compressive amplitude late in the fatigue life. After this point, a moderate decrease in compressive stress amplitude was observed. Hysteresis gradually increased during fatigue with markedly more hysteresis occurring on the tensile side of the stress/strain curve. Late in the fatigue life, the decrease in tensile stress amplitude with each loading cycle became very pronounced and a bend appeared in the recorded stress/strain curve. At failure the tensile stress amplitude was decreased to 64 percent (S.D. 15) of the initial value and the compressive stress amplitude was increased to 148 percent (S.D. 9) of the initial value (Figure 5).

Specimens tested with a compressive mean strain of −0.002 exhibited a small, abrupt decrease in compressive stress amplitude during the first five loading cycles. This was followed by a gradual and progressive loss in compressive stress amplitude during fatigue. A similar though less pronounced loss of tensile stress amplitude was observed. Hysteresis gradually increased during fatigue with more hysteresis occurring on the compressive side of the stress/strain curve than on the tensile side. Failure was preceded by an accelerated loss of compressive stress amplitude which was followed by an accelerated loss of tensile stress amplitude. At failure the tensile stress amplitude was decreased to 72 percent (S.D. 18) of its initial value and the compressive stress amplitude was decreased to 71 percent (S.D. 5) of its initial value.

DISCUSSION

Fatigue fracture

The results of this study indicate that bone has extremely poor fatigue resistance compared to most engineering materials. The mean tensile yield strain was found to be 0.0068 by the method of Reilly & Burstein and 0.0084 by the 0.2 percent offset method. Fatigue loading from a strain of −0.003 to +0.003 ($\Delta\varepsilon = 0.006$) caused failure of the specimens in about 2147 loading cycles (Figure 6). By comparison, fatigue loading in steel specimens to half of the yield strain would be below the endurance limit and thus would *never* cause fatigue failure. These findings demonstrate that the range of stresses and strains that bone tissue can tolerate *in vivo* without major damage is much smaller than has generally been assumed. The fatigue behavior of bone as shown in this study and the work of Carter & Hayes (1977a) & Carter & Hayes (1977b) is similar to that in many other composite materials which do not have an endurance limit. After reviewing all experimental studies that have been conducted to date, we feel that there is no indication of an endurance limit for bone.

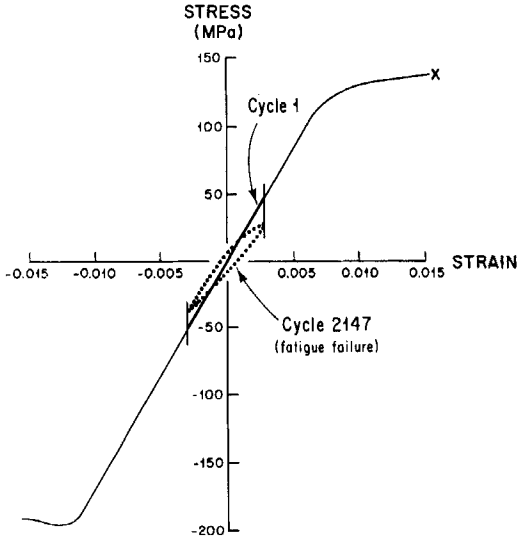

Figure 6. Schematic representation of bone fatigue with a mean strain of zero. A cyclic strain range of 0.006 leads to fatigue fracture after approximately 2147 cycles.

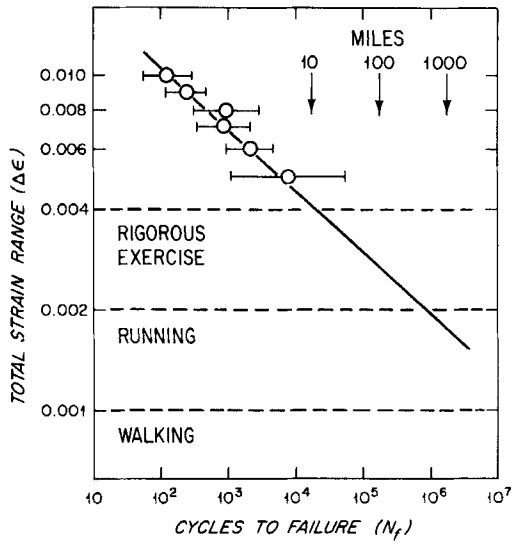

Figure 7. The fatigue data of this study (log mean ± S.D.) are plotted to allow comparisons with estimated strain ranges expected during various in vivo activities.

In estimating fatigue failure in bony structures, most previous investigators have emphasized the maximum stress or strain to which the tissue is exposed. Results of this study indicate that maximum stress or strain does not correlate well with the total number of cycles to fatigue failure. On the contrary, the fatigue life was independent of the maximum strain (or mean strain) and was determined only by the total strain range during testing.

The levels of strain employed in this study are higher than those normally experienced by bone *in vivo*. Since the tests were conducted at physiologic loading rates, it was impractical to fatigue the specimens at lower strain ranges because of time restraints. Results by Swanson et al. (1971) and Carter & Hayes (1976) and Lafferty (1978) at higher loading frequencies suggest, however, that fatigue data taken from specimens which fail in 10 to 10,000 cycles can be safely extrapolated out to at least 10^7 cycles to failure. In Figure 7, the fatigue results of this study are compared with the strain ranges which may occur in bone during *in vivo* activities. The estimates of *in vivo* strain range in Figure 7 are based on minimal experimental data. Bone strain during very rigorous activities has never been measured

in any animal. The only study which directly measured strain on a human bone *in vivo* was that by Lanyon et al. (1975). These investigators bonded a strain gauge rosette to the antero-medial aspect of the tibial midshaft of a 35-year-old man. Principal strains as a function of time were reported for walking (1.4 meters/second) and slow jogging (2.2 meters/second). By resolving these strains into axes which correspond to the axis of the tibia (Carter 1978) it can be shown that during slow jogging the axial mean strain was approximately +0.0003 and the strain range was 0.001. The loading was primarily tensile. Since there was negligible shear strain during jogging, these values are directly comparable to the fatigue specimens of this study. During walking the axial mean strain was near zero and the axial strain range was about 0.00037; however, there was a significant shear strain range of 0.0008 with a mean shear strain of 0.0004. The presence of shear strain (presumably due to torsion during gait) would tend to create additional fatigue damage to the bone and lower the estimate of fatigue life predicted by the results of the present study.

It is highly probable that the strain histories recorded by Lanyon et al. were not measured at the location of highest stress or strain. Higher tensile strains are probably experienced by bone on the anterior or antero-lateral surfaces. Additionally, since the midshafts of long bones are exposed to compressive forces and bending, the highest cyclic stresses and strains are in primarily compressive areas which were not measured in the human study by Lanyon et al.

Considerably more direct measurements of bone strain have been conducted in animals. In dogs walking at 1.4 meters/second, Carter et al. (1980) recorded axial mean strains of 0.0001 and strain ranges of 0.00065 on the cranial surface of the mid-radius. Significant shear strains were also recorded. Lanyon & Smith (1970) measured peak axial tensile strains during gait of approximately +0.0007 on the cranial aspect of sheep radii and peak compressive strains of –0.0012 on the caudal aspect. Turner et al. (1975) recorded axial mean strains of about –0.0005 and an axial strain range of 0.001 from the medial equine metacarpus during walking. During trotting the mean axial strain was approximately –0.00085 and the strain range was about 0.0017.

It is difficult to estimate the strain histories which may be encountered in humans during very rigorous activities. However, several investigators have estimated that reaction forces during rigorous activities may be three to five times greater than those in normal walking. The estimated strain range levels during exercise shown in Figure 7 are based on the assumption that cyclic strain ranges may show similar increases. Ongoing research in several laboratories will hopefully provide better estimates of *in vivo* bone strain ranges during strenuous activities. However, the data of Figure 7 are not inconsistent with clinical experience with fatigue fractures in military recruits and athletes (Devas 1975, Morris & Blickenstaff 1967). Military recruits may experience a fatigue fracture within 6 weeks after beginning rigorous training. In this time period, it would be possible to accumulate a loading history equivalent to 100 to 1000 miles of very rigorous exercise. This is roughly equivalent to 100,000 to 1,000,000 loading cycles. The fatigue data of this study predicts cyclic strain ranges of 0.0029 and 0.0019, respectively, for these fatigue fractures. The estimates ignore, of course, any influence of *in vivo* remodeling which may delay or accelerate *in vivo* bone fracture.

Fatigue damage accumulation and the biological response

The mechanical data collected during fatigue testing indicates that bone fatigue is accompanied by diffuse structural damage which manifests itself very early in the loading history. The specimens tested exhibited an almost immediate loss of bone stiffness and an increase in stress/strain hysteresis. These events indicate the presence of bone microdamage. The findings of this study further substantiate the results of Carter & Hayes (1977a) who found that during fatigue loading, internal damage was created in the bone structure which causes a gradual and progressive loss of bone stiffness and strength prior to catastrophic failure. Examination of the stress histories and stress/strain curves recorded in the present study indicate that specimens tested with a mean com-

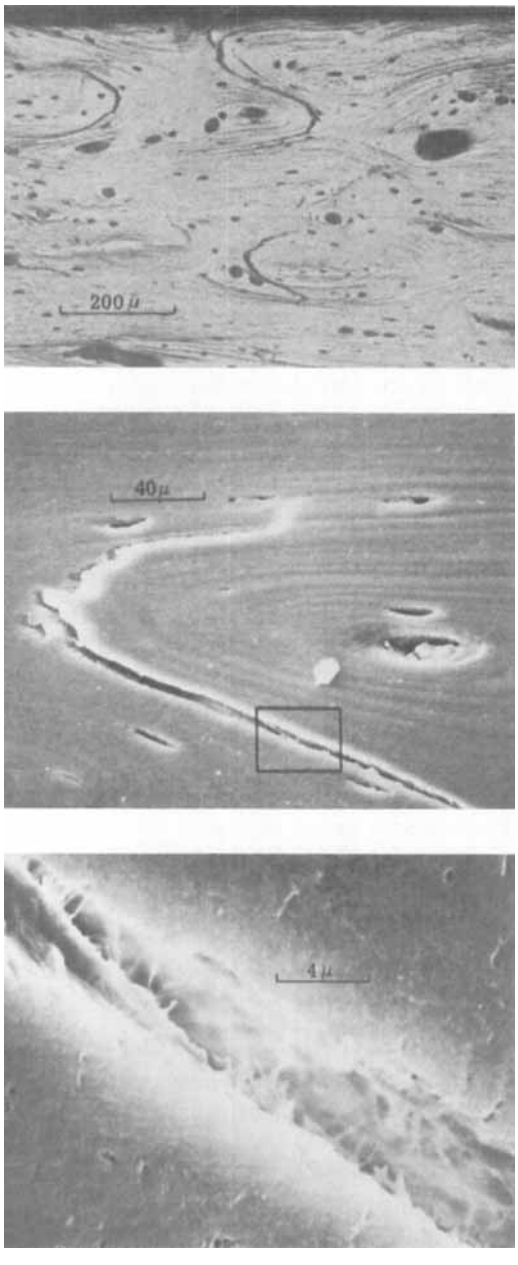

Figure 8A–C. (A, Top) Reflected-light photomicrograph of tensile fatigue damage. (B, Center) SEM photomicrograph depicting osteon debonding shown in (A). (C, Bottom) Higher magnification of osteon debonding area shown in (B) [from Carter & Hayes (1977b)].

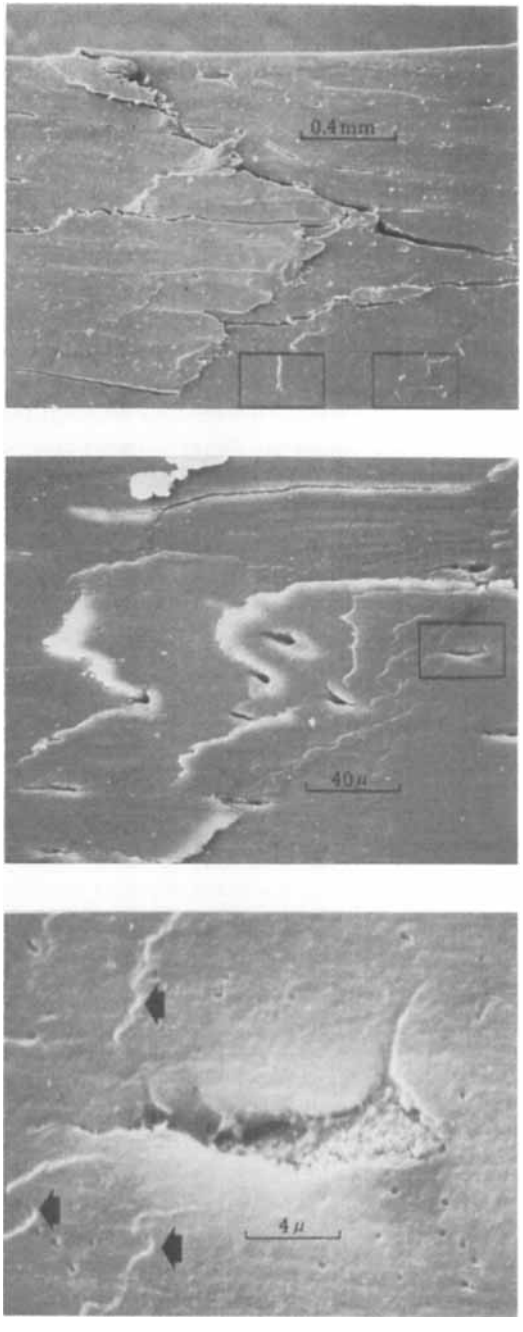

Figure 9A–C. (A, Top) SEM photomicrograph of compression fatigue damage. (B, Center) Compression microcracks in an area shown in (A). (C, Bottom) Microcrack near lacuna shown in (B) [from Carter & Hayes (1977b)].

pressive strain experienced a greater accumulation of damage in the compressive phase of the loading cycle (Figure 5). Specimens tested with a zero mean strain accumulated damage in both the tensile and compressive phases of the loading cycle, but more damage appeared to accrue during the tensile phase. Specimens tested with a tensile mean strain exhibited a much greater degree of damage in the tensile phase of loading.

The damage accumulation as shown by the mechanical events recorded in this study is related to specific structural defects created in the bone structure. Carter & Hayes (1977b) showed that the type of fatigue microdamage created is determined by the type of local stresses or strains which are imposed on the tissue. In bone tissue which accumulates tensile fatigue damage, there is extensive failure at the osteon cement lines and interlamellar cement bands (Figure 8). The nature of this damage is such that direct insult to bone cells and canaliculi is minimal. In bone tissue which accumulates compressive fatigue damage, numerous oblique microcracks are created (Figure 9). The formation of these microcracks appears to be influenced to some extent by the stress concentrations created by vascular canals and lacunae. Direct insult to bone cells and canaliculi is extensive.

Since the mechanical manifestations of fatigue damage in the present study were influenced by the mean strain, it is reasonable to assume that these manifestations are a reflection of the physical damage that has accumulated. One would expect that specimens tested with a mean tensile strain would accumulate more damage of the type reflected in Figure 8. Specimens tested with a mean compressive strain would accumulate more damage of the type shown in Figure 9, with a greater degree of insult to bone cells. The type of fatigue microdamage and consequently the degree of cellular insult is, therefore, dependent upon the mean strain. As the loading becomes more compressive, there is a greater degree of direct insult to bone cells and canaliculi. This observation is important when trying to relate the data of this study (which reflect only mechanical phenomena) to the *in vivo* fatigue situation which reflects both mechanical and biological processes. The more extensive cellular insult to bone cells during compressive fatigue loading may provide a greater stimulus for biological repair of microdamage and extend the *in vivo* fatigue life of bone. This possibility suggests that the *in vivo* fatigue resistance of bone may be influenced by the mean strain despite the fact that *in vitro* fatigue life is not.

The idea that a different cellular response may be illicited in areas of predominately tensile and predominately compressive microdamage is fully consistent with what is generally believed concerning the stress related remodeling response of bone. In cortical bone there is generally more bone deposition in areas of increased cyclic bone compression than in areas of increased cyclic bone tension. The predominate hypothesis for this differential response of bone to tensile and compressive stresses is based on the stress generated electric potentials in bone (Bassett 1972). Bone tissue in compression has been shown by numerous investigators to have a negative electrical potential with respect to the more positively charged tensile regions.

It has been shown that when electrodes are attached to cortical bone, more new bone is formed near the negatively charged cathode than around the positively charged anode. The microdamage hypothesis of the stress related remodeling response is fully compatible with the conventional theory of the stress generated potentials in bone. It is conceivable that both mechanisms work in a complementary fashion to regulate bone physiology over the entire range of *in vivo* bone strains. In a complementary process of bone regulation of this type, bone fatigue microdamage would probably have its most pronounced influence at the higher strain ranges where microdamage accumulation is most severe.

REFERENCES

Bassett, C. A. L. (1972) Biophysical principles affecting bone structure. *The biochemistry and physiology of bone.* (Ed. Bourne, G. H.), Academic Press, New York.

Baud, D. A. (1976) Histophysiology of the osteocyte: An introduction to the morphometry of peri-osteocytic lacunae. *Bone morphometry,* pp. 267–272, Univ. of Ottawa Press, Ottawa, Canada.

Carter, D. R. (1978) Anisotropic analysis of strain rosette information from cortical bone. *J. Biomech.* **11**, 199–202.

Carter, D. R. & Hayes, W. C. (1976) Fatigue life of compact bone I. Effects of stress amplitude, temperature and density. *J. Biomech.* **9**, 27–34.

Carter, D. R., Hayes, W. C. & Schurman, D. J. (1976) Fatigue life of compact bone II. Effects of microstructure and density. *J. Biomech.* **9**, 211–218.

Carter, D. R. & Hayes, W. C. (1977a) Compact bone fatigue damage I. Residual strength and stiffness. *J. Biomech.* **10**, 325–338.

Carter, D. R. & Hayes, W. C. (1977b) Compact bone fatigue damage: A microscopic examination. *Clin. Orthop.* **127**, 265–274.

Carter, D. R., Spengler, D. M. & Frankel, V. H. (1977) Bone fatigue in uniaxial loading at physiologic strain rates. *IRCS J. Med. Sci.* **5**, 592.

Carter, D. R. & Spengler, D. M. (1978) Mechanical properties and chemical composition of cortical bone. *Clin. Orthop.* **135**, 192–217.

Carter, D. R., Smith, D. J., Spengler, D. M., Daly, C. H. & Frankel, V. H. (1980) Measurement and analysis of *in vivo* bone strains on the canine radius and ulna. *J. Biomech.* **13**, 27–38.

Chamay, A. & Tschantz, P. (1972) Mechanical influences in bone remodeling. Experimental research on Wolff's law. *J. Biomech.* **5**, 173–180.

Devas, M. B. (1975) *Stress fractures.* Churchill Livingstone, London and New York.

Evans, F. G. & Lebow, M. (1957) Strength of human compact bone under repetitive loading. *J. Appl. Physiol.* **10**, 127–130.

Evans, F. G. & Riolo, M. L. (1970) Relations between the fatigue life and histology of adult human cortical bone. *J. Bone Joint Surg.* **52**-A, 1579–1586.

Freeman, M. A. R., Todd, R. C. & Pirie, C. J. (1974) The role of fatigue in the pathogenesis of senile femoral neck fractures. *J. Bone Joint Surg.* **56**-B, 698–702.

Gray, R. J. & Korbacher, G. K. (1974) Compressive fatigue behavior of bovine compact bone. *J. Biomech.* **7**, 287–292.

Johnson, T. A. (1973) Cyclic deformation and failure of polymers, cyclic stress-strain behavior-analysis, experimentation, and failure prediction. pp. 70–97. ASTM STP 519, American Society for Testing and Materials.

King, A. I. & Evans, F. G. (1967) Analysis of fatigue strength of human compact bone by the Weibull method. *Digest of the Seventh International Conference on Medical and Biological Engineering.* (Ed. Jacobson, B.), pp. 514. The Organizing Committee of the Conference, Stockholm.

Lafferty, J. F. (1978) Analytical model of the fatigue characteristics of bone. *Aviat. Space Environ. Med.* **49**, 170–174.

Lanyon, L. E., Hampson, W. G. J., Goodship, A. G. & Shah, J. S. (1975) Bone deformation recorded *in vivo* from strain gauges attached to the human tibial shaft. *Acta Orthop. Scand.* **46**, 256–268.

Lanyon, L. E. & Smith, R. N. (1970) Bone strain in the tibia during normal quadrupedal locomotion. *Acta Orthop. Scand.* **41**, 238–248.

Lease, G. O'D. & Evans, F. G. (1959) Strength of human metatarsal bones under repetitive loading. *J. Appl. Physiol.* **14**, 49–51.

Morris, J. M. & Blickenstaff, L. D. (1967) *Fatigue fractures.* Charles C. Thomas, Springfield, Ill.

Mueller, K. H., Trias, A. & Ray, R. D. (1966) Bone density and composition. *J. Bone Joint Surg.* **48**-A, 140–148.

Nash, C. D. (1966) Fatigue of self-healing structures. A generalized theory of fatigue failure. American Society of Mechanical Engineers. Publ # 66WA/BHF-3, New York.

Prather, J. L., Nusynowitz, M. L., Snowdy, H. A., Hughes, A. D., McCarthey, W. H. & Bagg, R. J. (1977) Scintigraphic findings in stress fractures. *J. Bone Joint Surg.* **59**-A, 869–874.

Radin, E. L. (1972) Trabecular microfractures in response to stress: The possible mechanism of Wolff's law. Orthopaedic surgery and traumatology. Proceedings of the 12th Congress of International Society of Orthopaedic Surgery and Traumatology, Tel Aviv, Oct. 9–12, pp. 59–65.

Reilly, D. T. & Burstein, A. H. (1975) The elastic and ultimate properties of compact bone tissue. *J. Biomech.* **8**, 393–405.

Salkind, M. J. (1972) *Composite materials: Testing and design.* American Society for Testing and Materials, Philadelphia, 497: 143.

Swanson, S. A. V., Freeman, M. A. R. & Day, W. H. (1971) The fatigue properties of human cortical bone. *Med. Biol. Eng.* **9**, 23–32.

Timoshenko, S. & Young, D. H. (1968) *Elements of strength of materials* (Ed. Van Nostrand, D.) New York.

Turner, A. S., Mills, E. J. & Gabel, A. A. (1975) *In vivo* measurement of bone strain in the horse. *Am. J. Vet. Res.* **36**, 1573–1579.

Underwood, E. E. (1970) *Quantitative stereology,* Addison-Wesley, Reading MA.

Correspondence to: Dennis R. Carter, Orthopaedic Research Labs, Massachusetts General Hospital, Boston, MA 02114, USA.